Study of the Fillers Influence on Mechanical Properties of Polyamide by Using of AFM

Dana Bakošová
Faculty of Industrial Technologies in Púchov, Alexander Dubček University of Trenčín. I. Krasku 491/30, 020 01 Púchov. Slovakia. E-mail: dana.bakosova@fpt.tnuni.sk

The works deals with a study of fillers influence on chosen mechanical properties of polyamide and the given influence was investigated by using of atomic force microscopy (AFM). Atomic force microscope NT-206 in a complex with control and image processing software is intended for measurement and analysis of surface microrelief and submicrorelief, objects of the micrometer and nanometer range with high resolution. Using AFM it is possible to scan spectroscopic curves that show dependence of composite action force of the probe and surface of the sample on distance between them – they are curves of approach /moving off. In presented measurements by using of spectroscopic curves, the homogeneity and ratio of Young's modulus for polyamide samples were evaluated. For each sample, the curve was created by using of five different places – points. We employed the general approximation and Snedonn's formula for analysis of data and calculation of Young's modulus off complete rake curve. The Sneddon's model gives the relationship between load gradient dP/dh and Young's modulus E.

Keywords: Polyamide, AFM, Spectroscopic curve, Sneddon's model, Young's modulus

1 The Properties of Polyamide

Polyamide is a semi crystalline thermoplastic with low density and high thermal stability. Polyamides are among the most important and useful technical thermoplastics due to their outstanding wear resistance, good coefficient of friction, and very good temperature and impact properties. In addition, polyamide exhibits very good chemical resistance and is an especially oil resistant plastic. This excellent balance of properties makes the PA polymer an ideal material for metal replacement in applications, such as automotive parts, industrial valves, railway tie insulators and other industry uses, whose design requirements include high strength, toughness and weight reduction. Polyamide shows a propensity to absorb moisture and thus has poorer dimensional stability than other engineering plastics. A distinction is made between two types. Polyamides made of one basic material (e.g. PA 6) and polyamides, which are made of 2 basic materials (e.g. PA 66). Properties vary from the hard and tough PA 66 to the soft and flexible PA 12. Furthermore, there is a distinct difference between polyamide shapes produced by extrusion, injection moulding and those produced by casting. Extrusion typically provides for smaller, higher volume machined parts, while casting typically allows for low volume, larger parts containing lower levels of internal stress. Injected, extruded and cast polyamides can be modified through the use of fillers to enhance certain properties (glass fiber, carbon fiber, mineral and or advanced fillers). With injection moulding, polyamide is sometimes filled with a certain percentage of glass fibers in order to increase its tensile strength. The percentage of glass is typically between 10% and 40%. The hooks we are injection moulding are actually above 40%. The glass fibers do increase strength, but they also impact the way a part fails. With no glass fill, polyamide will bend and yield before it breaks. With the addition of the glass fibers (especially at higher percentages), the failure becomes an instantaneous brittle break with very little bending. When polyamide has a glass fiber fill it is referred to as, for example, GF 20 polyamide. When polyamide has a carbon fiber fill it is referred to as, for example, CF 20 polyamide. Polyamide can be readily machined and is able to provide a full range of secondary machining operations, such as turning, drilling, tapping and grinding, as well as ultrasonic insertion, ultrasonic welding, pad printing and assembly. The natural color of polyamide is a milky white which lends itself to easily being changed via the addition of color concentrates or selecting a precolored resin. Polyamides for injection moulding and extrusion include PA 6 grades, PA 66 grades as well as special polyamides such as partially aromatic polyamides mainly 6T based, PA6.10, PA6.12, PA11, PA12, PA46, etc. [1], [2].

2 Atomic-force microscope

Atomic-force microscope (AFM NT-206 - Fig. 1) in a complex with control and image processing software is intended for measurement and analysis of surface microrelief and submicrorelief, objects of the micrometer and nanometer range with high resolution [3]. Fields of application of the AFM include physics of solids, thin-film technologies, nanotechnologies; microtribology and nanotribology, microelectronics, optics, testing systems of the precision mechanics, magnetic record, vacuum engineering etc. The AFM can be used in scientific and industrial laboratories. The image of a surface by the AFM is obtained through scanning of a sample in a horizontal plane by a tip attached to the cantilever and this tip has the curvature radius about tens–hundreds of nanometers. A control system traces the probe position relative to the sample surface in every measurement point and it also adjusts the tip to sample separation at constant level set by the operator. The changes of the probe vertical position in every point lead to the AFM data matrix which is recorded in a file and then can be used for further processing, visualization and analysis [4].

The scanning unit (Fig. 1) is designed for work in open air and gives convenient access for sample installa-

tion and change of scanning probe. The instrument employs measuring scheme with stationary probe over the movable sample. During measurements, precision movements of the sample are provided by a tube piezoscanner on which the sample is placed. Before measurements, the position of the probe has to be adjusted over sample to target necessary area using motorized positioning stage. The scanning unit comprises base platform (case) (1) and detachable measuring head (8). All mechanisms are assembled on the case upper plate that serves as a base plate. On lower side (inside the case), there is a mechanism of the piezoscanner vertical motion on the base plate. The mechanism provides the approach (lifting) and the withdrawal (lowering) of the piezoscanner in relation to the sample placed on sample platform established on the tube top (16) relating to the probe (Z or vertical motion). Range of the mechanism motion is from 20 mm with the step down to about 200 nm. On the upper side of the base plate, the XY positioning stage is mounted and it is used for preparatory motion of the measuring head over the sample (coarse XY positioning) to target necessary area on it. The positioning stage consists of Y stage (2) with its driving stepper motor (3) and X stage (4) with own driving stepper motor (5). The XY positioning stage motion range is 10 mm in both directions with step 2.5 micron. From above, the X positioning stage, a dove tale (6) is mounted for installation of the measuring head (8). The measuring head (8) is installed by moving it forward from the front in horizontal plane. Screw (7) serves for tight fixing of the measuring head on base platform. To switch the measuring head into the general circuit, it is necessary to plug its cable (20) into socket on the rear side of the case. Additionally, it is necessary to plug the USB cable (21) of the video camera (18) into free USB socket on the host computer. To detach the measuring head from the base platform (case), the connectors (from measuring head and from video camera) have to be unplugged, the fixing screw has to be unscrewed (7) and the head off the dove tail has to be pulled (6). Measuring head (8) represents a high-precision system comprising mechanical, optical and electronics equipped with specially designed video camera (18). In the lower part of the measuring head, a removable probe holder (12) is installed. Screw (13) is used for locking the probe holder after installation it in the measuring head. Knobs (9) and (10) serve for targeting the laser beam on to the probe at tuning. It is important to say that laser source and video camera optics are integrated in one system and therefore video camera (18) moves with the laser source adjustment. This scheme provides permanent targeting of the video camera on to the area around the laser beam center. Knobs (14) and (15) are used for tuning the photodetector on to the beam reflected from the rear side of the probe cantilever. Axis (11) turns a mirror reflecting the bounced beam on to the photodetector and can be used for additional tuning of the measuring system (it is, however, recommended to keep this axis as it was established by the manufacturer and use this option in extreme cases). Ring (19) on the video camera tube (17) serves for fine focusing of the video system in the range about 1 mm along vertical axis. The video camera module (18) can be detached from the system by unfixing special screw on the tube and pulling it then up. The video system contains fine optical elements inside and therefore it is strongly recommended to protect the opened ends of the tubes against dust and dirt.

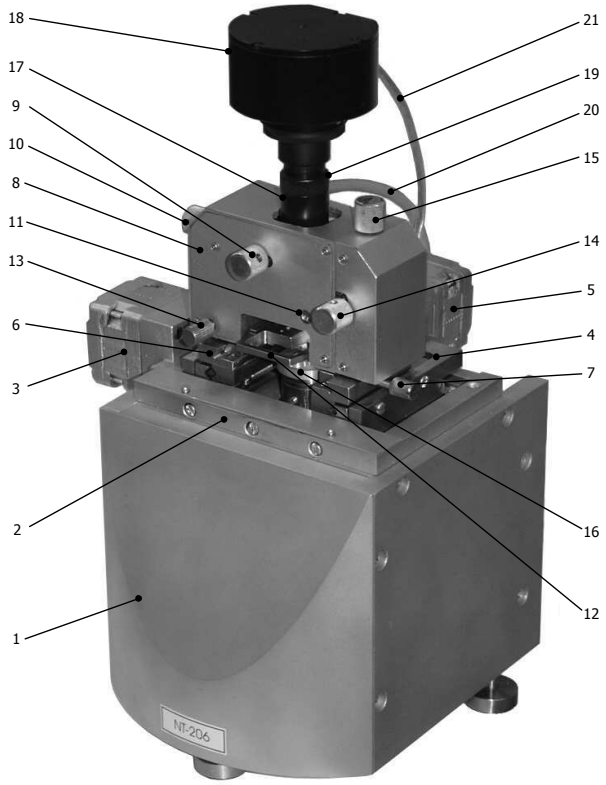

Fig. 1 *Scanning unit of atomic force microscope NT-206*

3 Utilization of atomic-force microscope

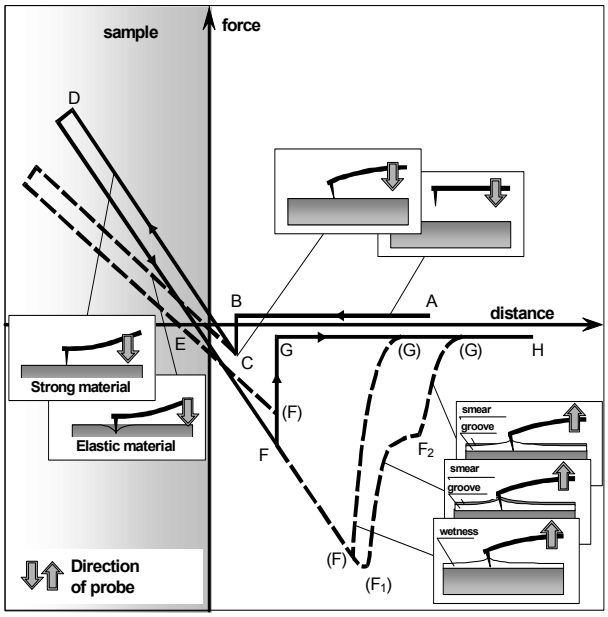

Fig. 2 *Nomograph of the approach/moving-off curves. The solid lines are schematic presentation of curves obtained in vacuum. Dashed lines show variations of curves of approach/moving-off subjected to elastic features of the sample as well as presence of surface layers of moisture and impurities [4], [5]*

Using AFM, it is possible to scan curves that show dependence of interaction of the probe composite force and surface of the sample relating to distance between them – they are curves of approach/moving off. These curves are very important for measurements of vertical force attached to the surface from the side of the tip in the process of scanning. Besides the force, it is also possible to evaluate viscosity of dirty surface, thickness of the covering layer and also local variations of elastic properties of the surface from the curve. The curves of approach/moving off that are obtained seem to be specific for each sample enough and at the same time we can separate general characteristic sections in them, as shown in Fig. 2 [5].

Section A – B: In the left part of the curve there is a scanning device completely moved off and the cantilever is not bent because the tip is not in the contact with the sample. By approaching the surface, the cantilever is not bent until the Van der Waals forces start to act (point B). In this part the curve does not contain any useful information.

Section B – C: In point B, the cantilever suddenly starts to move towards the surface and the tip starts to be in a contact with the surface (point C). This part of the curve is known as "leap to contact". Besides Van der Waals attractive forces and electrostatic forces, there is a compound influence of the surface moisture capillarity as well as impurities and grease on the tip during the working in air environment. Change of the force in the part B – C of the curve can be related to the tip shrinkage in accordance with the Hook law ($F = -k\Delta x$) and it allows to evaluate the thickness of absorbed layer on the sample surface.

Section C – D: This part characterizes further approach of the probe to the sample and it is accompanied by driving needle tip to the surface and moreover there is nearly linear curve of the cantilever towards the surface. From the shape of the C – D section, we can evaluate modulus of elasticity of the system probe – surface. In the case that, for example, the measuring probe is much softer than the surface of the sample, the curve inclination presents mostly elastic constant of the cantilever itself. Contrariwise, if the hardness of the cantilever is much harder than the surface of the sample, inclination of the section C– D allows us to study elastic features of the sample. Section C – D does not have to be straight line at all, the inclination change of this curve part shows differences in surface reactions to different attached force.

Section D – E: Point D refers to the end of the approaching phase and the beginning of moving-off phase from the surface. If there is not hysteresis of the scanning device, the section D – E is practically the same as the section of the curve C – D, which we obtained during the approach. In the case that both of these sections are straight and parallel they do not give us any additional information (besides above mentioned). In the case that they are unparallel it allows us to determine plastic and elastic deformation of the sample (if the speed of recovery of surface geometrical features is slower than moving-off of the probe).

Section E – F: Point E refers to the neutral divergence of the cantilever. During further moving-off of the probe from the surface, the cantilever starts to incline to the sample because adhesive or gravity force affects the tip. The shape of the section E – F is influenced by presence of absorbing layers on the sample surface. In the case of the work in vacuum, Van der Waals and electrostatic forces affect the tip of the needle. If we work at the air conditions, quite strong capillary force of moisture on surface layer, grease and impurities are added to these forces. Thickness of the surface layer influences the length of the section E – F and its inclination, which is different to inclination caused by hardness of the sample, and points to moving up absorbing layers together with the moving-off probe. When the elastic response of the cantilever outruns gravity forces of the surface side and its layers, the probe separates from the sample surface. Point F, known as the point of separation, refers to this action in the curve of approach/moving off.

Section F – G: When the elastic response of the cantilever outruns the gravity force of the surface and its layers, the probe separates from the sample. In the curve of approach/moving-off there is a point *F*, known as the point of separation, referring to this mentioned above. The size of straining in the point *F* is equal to the total maximum adhesive force between the probe and sample and provides key information on observation of adhesion. If the moisture layer is covered enough with grease layer or other impurities, it is the case when we can observe not only one point of separation (F_1 and F_2). Position of the points F_1 and F_2 depends on viscosity and thickness of these layers. Transition between the sections E – F and F – G does not necessarily have to have steep ascent. In the case that the absorbing layer has equal viscosity, the probe can move off from the surface gradually and the transition E – F, F – G will have round shapes [6], [7].

4 Experiment

In presented measurements by using of spectroscopic curve, the homogeneity and ratio of Young's modulus were evaluated for PA samples. The PA samples were:

- **Polyamide PA 6 BT -** basic type PA 6 for injection moulding, modified for general use, with excellent manufacturing properties. Use: automotive, engineering, electrical and consumer-goods industry - electrical tools, fasteners, clamps, hobby tools, toys.
- **Polyamide PA 6 GF 20 -** PA 6 for injection moulding, chemically strengthened with 20% glass fibre, heat stabilized . Application: impacted mouldings and mouldings with high strength applied in automotive, electrical, engineering and consumer-goods industry, e.g.: grips for electro tools, hobby tools, gears, cases of the electrotools, cooling skrews of blowers, electromotors, carrying parts in the automotive industry. With the increasing content of GF also the toughness, bending and tensile strength

increase as well as the heat application increases up to 250°C and the shrinkage decreases.

- **Polyamide PA 6 CF 20 -** Chemically reinforced with 20 % carbon fibre, suitable for mouldings with high strength and toughness also at minus temperatures. Used in the automotive, engineering and electrical industry. Application: hobby tools, covers of electrotools, electromotors, cooling screws of blowers, gear wheels, carrying parts in the automotive industry like e.g. brake cables.

For each sample, the curve by using of five different places - points was created. In Figs. 3, 4, 5 there is the presentation of examples relating to the spectroscopic curves for investigated samples. In Fig. 6, 7, 8 the surface topography of investigated samples is presented.

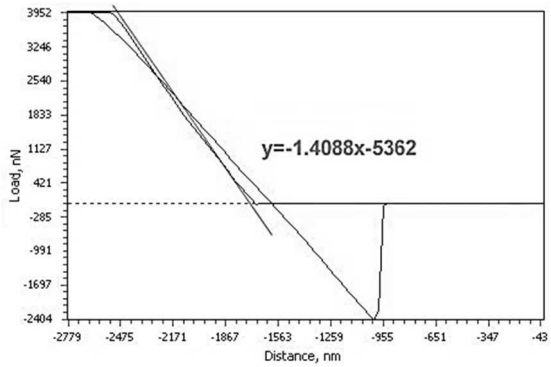

Fig. 3 *Spectroscopic curve - Polyamide PA 6 BT*

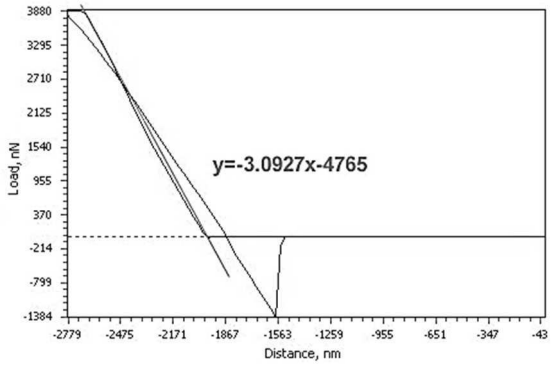

Fig. 4 *Spectroscopic curve - Polyamide PA 6 GF 20*

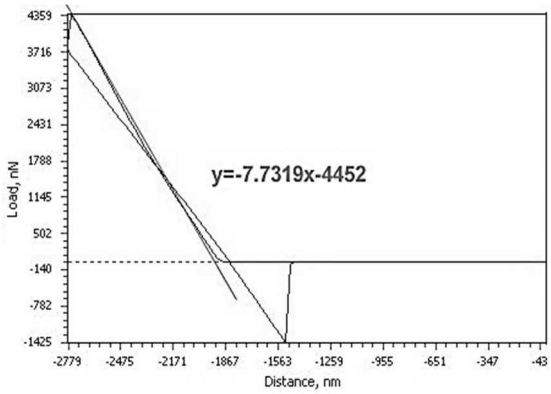

Fig. 5 *Spectroscopic curve - Polyamide PA 6 CF 20*

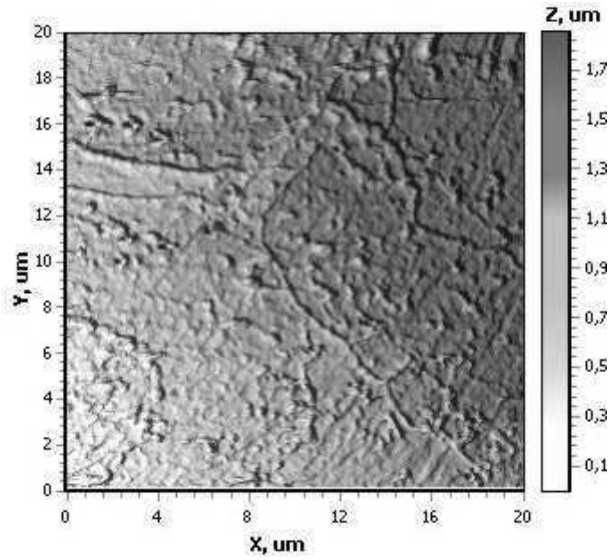

Fig. 6 *Topography of microsurface of sample - Polyamide PA 6 BT*

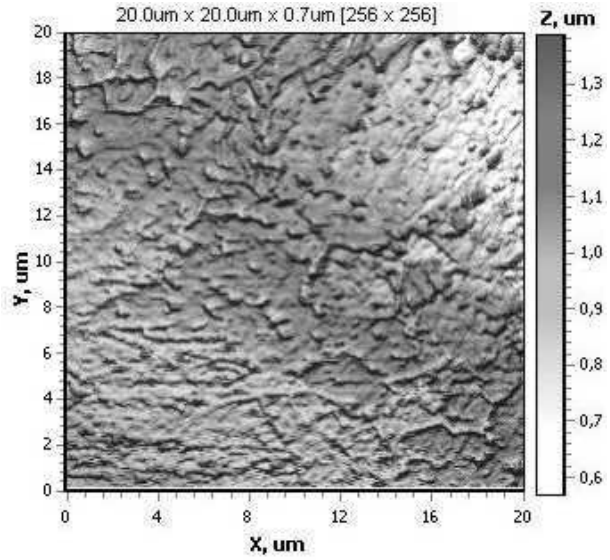

Fig. 7 *Topography of microsurface of sample - Polyamide PA 6 GF 20*

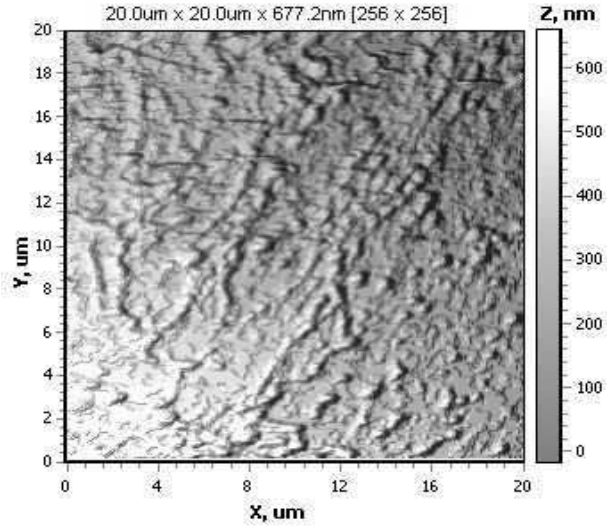

Fig. 8 *Topography of microsurface of sample - Polyamide PA 6 CF 20*

We employed the general approximation and Sneddon's formula for analysis of data and calculation of Young's modulus of complete rake curve. The Sneddon's model gives the relationship between load gradient *dP/dh*, and Young's modulus *E* in the form [5]:

$$\frac{dP}{dh} = \frac{2A^{1/2}}{\pi^{1/2}} E, \tag{1}$$

where

$$E = \left\{\left[\left(1-\nu_m^2\right)/E_m\right] + \left[\left(1-\nu_c^2\right)\right]/E_c\right\}^{-1}\left[Pa\right], \tag{2}$$

is the compound elastic modulus, (E_m, E_c, ν_m, ν_c Young's modulus and Poisson's ratio of a material and a cantilever, respectively), *P* is normal load [*N*], *A* is contact area [m^2], *h* is the indentation depth [*m*]. Provided we can assume $E_c >> E_m$, and therefore $E = E_m$.

The following formula 1 represents the modulus of two different samples:

$$\frac{dP_1}{dh_1} = \frac{2A^{1/2}}{\pi^{1/2}} E_1 \Rightarrow E_1 = \frac{dP_1}{dh_1}\frac{\pi^{1/2}}{2A^{1/2}}, \tag{3}$$

$$\frac{dP_2}{dh_2} = \frac{2A^{1/2}}{\pi^{1/2}} E_2 \Rightarrow E_2 = \frac{dP_2}{dh_2}\frac{\pi^{1/2}}{2A^{1/2}}. \tag{4}$$

The relation of modulus of elasticity:

$$\frac{E_1}{E_2} = \frac{\frac{dP_1}{dh_1}\frac{\pi^{1/2}}{2A^{1/2}}}{\frac{dP_2}{dh_2}\frac{\pi^{1/2}}{2A^{1/2}}} \Rightarrow \frac{E_1}{E_2} = \frac{\frac{dP_1}{dh_1}}{\frac{dP_2}{dh_2}}. \tag{5}$$

The linear equation is:

$$y = kx + q \text{, where } k = \frac{dP}{dh}, \tag{6}$$

$$\frac{dP_1}{dh_1} = k_1 \text{ and } \frac{dP_2}{dh_2} = k_2, \tag{7}$$

$$\Rightarrow \frac{E_1}{E_2} = \frac{k_1}{k_2}. \tag{8}$$

The equations of line were obtained from spectroscopic curves by approximation and resulting values are presented in the tab. 1.

Tab. 1*The values of k1 , k2 and k3 obtained by approximation of spectroscopic curves by assignation of line*

k_{1-1}	k_{1-2}	k_{1-3}	k_{1-4}	k_{1-5}	k_1
-1.4088	-1.4102	-1.4095	-1.4109	-1.4099	**-1.4099**
k_{2-1}	k_{2-2}	k_{2-3}	k_{2-4}	k_{2-5}	k_2
-3.0927	-3.0935	-3.0931	-3.0917	-3.0913	**-3.0925**
k_{3-1}	k_{3-2}	k_{3-3}	k_{3-4}	k_{3-5}	k_3
-7.7319	-7.7328	-7.7301	-7.7325	-7.7302	**-7.7315**

By using of average values:

- k_1 = -1.4099 Polyamide PA 6 BT,
- k_2 = -3.0925Polyamide PA 6 GF 20,
- k_3 = -7.7315Polyamide PA 6 CF 20.

They are presented for the comparing of sample moduli:

$$E_2 = \frac{k_2 E_1}{k_1}\left[Pa\right], \tag{9}$$

$$E_3 = \frac{k_3 E_1}{k_1}\left[Pa\right], \tag{10}$$

where

- E_1 – Young's modulusPolyamide PA 6 BT,
- E_2 – Young's modulusPolyamide PA 6 GF 20,
- E_3 – Young's modulusPolyamide PA 6 CF 20.

The following formulas 9 and 10 represents ratio the modulus of PA samples:

$$\Rightarrow E_2 = \frac{k_2 E_1}{k_1} = \frac{-3.0925}{-1.4099} E_1 \qquad \underline{\Rightarrow E_2 = 2.1934 E_1\left[Pa\right]},$$

$$\Rightarrow E_3 = \frac{k_3 E_1}{k_1} = \frac{-7.7315}{-1.4099} E_1 \qquad \underline{\Rightarrow E_3 = 5.4837 E_1\left[Pa\right]}.$$

5 Conclusions

From spectroscopy curves and following calculations, it can be concluded that Young's modulus of the Polyamide PA 6 GF 20 sample with glass fibre is the 2.1934 times higher than Young's modulus of basic type Polyamide PA 6 BT and Young's modulus of the Polyamide PA 6 CF 20 sample with carbon fibre is the 5.4837 times higher than Young's modulus of basic type Polyamide PA 6 BT. Materials with a high Young's Modulus are stiffer than materials with lower Young's Modulus. We can allege that the PA with glass fibre or carbon fibre has the reinforcing effect. A high modulus of elasticity is sought when bending or deflection is not wanted, while a low modulus of elasticity is required when flexibility is needed. From these surface topography and spectroscopic

curve inclination, it is possible to say that all used samples are homogeneous.

Acknowledgement

This paper deal was supported by the Slovak Grant Agency KEGA 007TnUAD-4/2017, VEGA grant No. 1/0649/17 and resulted from the project "Center for quality testing and diagnostics of materials", ITMS code 26210120046 relating to the Operational Program Research and Development funded from European Fund of Regional Development.

References

[1] MULLER, M., VALASEK, P. (2012). Abrasive wear effect on Polyethylene, Polyamide 6 and polymeric particle composites. *Manufacturing Technology*, Vol. 12, No. 12, pp. 55-59.

[2] VALASEK, P., MULLER, M. (2012). Polymeric particle composites with filler saturated matrix. *Manufacturing Technology*, Vol. 12, No. 13, pp. 272 – 276.

[3] WIESENDANGER, R. (1994). *Probe Microscopy and Spectroscopy: Methods and Applications*. Cambridge University Press.

[4] WEISENHORN A.L., HANSMA P.K., ALBRECHT T.R., QUATE C.F. (1989). Forces in Atomic Force Microscopy in Air and Water. *Appl. Phys. Lett*. Vol. 54, No. 26, pp. 2651–2653.

[5] CHIZHIK, S. A.,GORBUNOV V. V. ,TSUKRUK V. V. , HUANG Z. (1998). Probing of micromechanical properties of compliant polymeric materials. *Journal of materials science*, No. 33, pp. 4905 – 4909.

[6] HUTTER J.L., BECHHOEFER J. (1994). Measurement and manipulation of Van der Waals forces in atomic force microscopy. *Journal of Vacuum Science and Technology*, No. 12, pp. 2251–2253.

[7] SUSLOV, A.A., CHIZHIK, S.A. (1997). Scanning Probe Microscopes. *Materials of Technology, Tools*, No. 3, pp. 78-79.

10.21062/ujep/73.2018/a/1213-2489/MT/18/2/173